

## VIBRATIONAL SPECTRA OF METHYLAMMONIUM IODIDE AND FORMAMIDIINIUM IODIDE IN A WIDE TEMPERATURE RANGE

Miha Bukleski\*, Sandra Dimitrovska-Lazova, Slobotka Aleksovska

Institute of Chemistry, Faculty of Natural Sciences and Mathematics, Ss. Cyril & Methodius University, Arhimedova 5, 1000 Skopje, Republic of N. Macedonia

mihabukleski@yahoo.com

Transmission infrared, Attenuated Total Reflectance (ATR) and Raman spectra of crystalline methylammonium iodide (MAI) and formamidinium iodide (FAI) in the temperature interval starting from  $-170\text{ }^{\circ}\text{C}$  to  $200\text{ }^{\circ}\text{C}$  were studied. The spectra recorded in the region from  $4000$  to  $500\text{ cm}^{-1}$  enabled resolving the ambiguities associated with the origin of some bands. For the first time a complete and detailed vibrational investigation and assignment of the IR spectra of these compounds based on the differences in the temperature dependent IR spectra for all phases have been made. The findings support the already established crystal structure of the phases for both compounds. The correlation between the overtones and fundamental modes has been confirmed based on the temperature induced isosbestic point.

**Keywords:** vibrational spectra; methylammonium iodide; formamidinium iodide; phase transition

### ВИБРАЦИОНИ СПЕКТРИ НА МЕТИЛАМОНИУМ ЈОДИД И ФОРМАМИДИНИУМ ЈОДИД ВО ШИРОК ТЕМПЕРАТУРЕН ИНТЕРВАЛ

Изучувани се трансмисионите, рефлексивните (придушена тотална рефлексивност – ATR) и раманските спектри на кристалните супстанции метиламониум јодид (MAI) и формамадиниум јодид (FAI) во температурниот интервал од  $-170\text{ }^{\circ}\text{C}$  до  $200\text{ }^{\circ}\text{C}$ . Снимените спектри во спектралната област од  $4000$  до  $500\text{ cm}^{-1}$  овозможуваат решавање на нејаснотиите поврзани со потеклото на некои ленти. За прв пат е направена целосна и детална вибрациона анализа и асигнација на инфрацрвените спектри на сите фази. Резултатите ги поткрепуваат веќе утврдените кристални структури кај двете соединенија. Потврдена е и поврзаноста на овертоновите и фундаменталните премини врз основа на температурно дефинираната изобестичка точка.

**Клучни зборови:** вибрациони спектри; метиламониум јодид; формамадиниум јодид; фазни премини

#### 1. INTRODUCTION

Even though methylammonium iodide ( $\text{CH}_3\text{NH}_2\text{I}$ , MAI) and formamidinium iodide ( $\text{CH}(\text{NH}_2)_2\text{I}$ , FAI) have very simple structures, their properties have not been subject to vast investigations. In the last few years, there is considerably an increased interest [1–4] since they have become some of the precursors for synthesis of novel

hybrid organic-inorganic perovskites (HOIPs). There are only few known organic cations that can successfully be incorporated in the HOIPs structure. Some of the perovskite properties are a direct consequence of the presence of the organic cation. For example, the improvement of the optoelectronic properties is directly influenced by the bandgap that depends on the type of the organic cation.

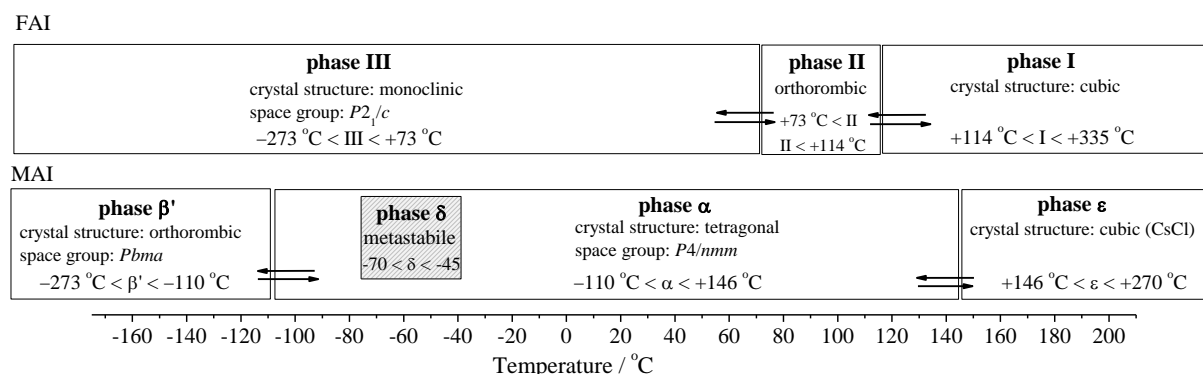
A systematic study of the infrared spectra of solid methylammonium halides has been carried out long time ago [5–8]. Even though the work is quite comprehensive, data about the high temperature phase of MAI are missing. As stated by Cabana and Sandorfy [5], the problem for not conducting the analysis above 22 °C is due to signs of decomposition of MAI. Also, the assignation of some of the bands is questionable. By making a detailed investigation about the changes in the spectrum as a function of temperature, one can follow the band evolution and band shift, so an unambiguous conclusion regarding the band assignment can be made.

The situation with formamidinium halides (FAX) is even more problematic. There are no thorough studies done on these compounds. The only information available are those obtained in the investigation of the HOIPs where FAX are used as precursors. Even in these papers, IR analyses are lacking, incomplete [9], or inaccurate [10]. More detailed assignation has been provided recently by Hills-Kimball et al. [11] but in this case only the

spectra at two temperatures have been covered (300 K and 350 K), so the phase transitions have not been studied.

Working in the field of synthesis of novel HOIPs, it was decided to examine the vibrational properties of one of the most promising organic cations for that purpose: MA<sup>+</sup> and FA<sup>+</sup>, in the form of iodides. Even though they seem simple and the assignation of the bands in the IR and Raman spectra should be straightforward, it was shown that the situation is complicated since both of them exist in different phases depending on the temperature. The structural characterization of the different phases has been previously reported [11–15], which can assist the process of assignation.

Three stable phases are known to exist in the temperature range from –170 °C up to the melting point of MAI and FAI. That suggests presence of two phase transitions in each compound. Based on the literature data [8, 11, 13, 15], the space group parameters as well as the temperatures of the transitions of MAI and FAI are given in Scheme 1.



**Scheme 1.** Distribution of the phases with structural characteristics and phase notation in the entire temperature range from absolute zero to the melting point of the compound

## 2. EXPERIMENTAL

### 2.1. Instrumentation

The IR absorption spectra were recorded on a Perkin-Elmer System 2000 FTIR Spectrometer using Liquid Nitrogen Cell (LNC). For the absorption measurements, KBr pellet technique was used. The absorption spectra were recorded with resolution of  $2\text{ cm}^{-1}$ , using 32 scans (both for the background and the sample spectra) in the temperature range starting from –170 °C up to 200 °C and again down to room temperature on the same pellet. The CO<sub>2</sub>/H<sub>2</sub>O software compensation was used in order

to reduce the bands intensity originating from the atmospheric moisture and the CO<sub>2</sub>.

The ATR spectra were recorded on the same Perkin-Elmer System 2000 FTIR Spectrometer using Golden Gate diamond ATR accessory with KRS-5 optics from Specac. The spectra were recorded in the reflectance mode and in the temperature range starting from room temperature (30 °C) up to 200 °C and again down to room temperature on the same sample setting. The recording was conducted with resolution of  $2\text{ cm}^{-1}$ , using 32 scans (both for the background and the sample spectra). The entire system (detector, sample compartment, ATR cell) was purged with dry nitrogen (99.999 %).

All IR spectra (both transmission and ATR) were recorded with five degree interval of the

temperature change between two spectra. Additionally, one degree temperature difference was set in order to record the temperature in the vicinity of the phase transition.

Raman spectra of the corresponding samples were recorded on a MicroRaman 300 from Horriba Jobin-Yvon. The spectra were recorded employing the red He-Ne 633 nm laser line, and the green Nd-Yag 532 nm laser line. Long-distance  $\times 50$  lens (Olympus) was used as an objective in both cases. The maximum power on the sample for 633 nm was 6.43 mW, while for 532 nm was 2.2 mW. In case of the 633 nm line, a D0.3 filter was used to lower the intensity. The integration time employed was 80 s, 180 s or 240 s, using two or four cycles for the Raman shift from  $100\text{ cm}^{-1}$  to  $4000\text{ cm}^{-1}$ . A diffraction grid with 1800 grooves/mm was used.

## 2.2. Synthesis

All chemicals used for the synthesis were with purity grade "for synthesis" and were used as received. The concentrated hydroiodic acid (57 %, w/w) was purchased by Carlo Erba Reagents with 1.5 %  $\text{H}_3\text{PO}_2$  as stabilizer, the methylamine aqueous solution (40 %, w/w) was purchased by Merck Millipore while the formamidinium acetate (99 %, w/w) was purchased from Sigma-Aldrich Company.

The synthesis of methylammonium iodide is rather straightforward [16]. Minor modifications suggested by the authors contributed to more stable product and have been previously described [17]. The MAI was synthesized using methylamine water solution and concentrated HI. The product was not further purified since both the XRD and IR results showed no impurities except from the  $\text{H}_3\text{PO}_2$  used as stabilizer of the HI.

The synthesis of the formamidinium iodide and its purification have been previously reported [17, 18]. As described, the synthesis was performed at  $0\text{ }^\circ\text{C}$  in ethanol solution of formamidinium acetate while adding the concentrated HI drop wise. The obtained product was recrystallized twice from methanol and diethyl ether mixture.

The characterization of both MAI and FAI was done by XRD powder diffraction. The results confirmed the successful synthesis of the compounds and their purity.

## 3. RESULTS AND DISCUSSION

The recorded IR and Raman spectra of both MAI and FAI at room temperature are in accordance with the already reported literature results [5, 7, 8, 11, 19]. For clarity and systematization of the assignation, parallel comparison of MAI and FAI

was applied in every region. The assignation is made for all stable phases. A key moment in the process of the assignment of the vibrational modes are the phase transition points where one can see the drastic changes in the appearance of the spectra. So far in literature the assignation has been made on a temperature at which the existence of a certain phase has already been established by XRD [12] or by other means [8, 13, 20]. In some cases this approach can lead to a wrong assignment of the bands [5, 21]. The reason can be the relatively close values for the wavenumbers of some bands. Additionally, when the evolution of the bands as a function of temperature, is not available improper assignation can be made.

The symmetry of the isolated  $\text{MA}^+$  ions is  $C_{3v}$  (Fig. 1) and if simple group theory considerations of this point group are taken into account than it can be concluded that there are five totally symmetric vibrations  $A_1$ , six doubly degenerated vibrations  $E$  and one  $A_2$  vibration that is non-degenerated and not totally symmetric. On the other hand, the point group of the isolated  $\text{FA}^+$  ion is  $C_{2v}$  (Fig. 1), having 18 internal modes. Seven of them are totally symmetric vibrations  $A_1$ , two that are not totally symmetric  $A_2$ , six of the  $B_1$  type and three that are  $B_2$ . All of them are non-degenerate vibrations.

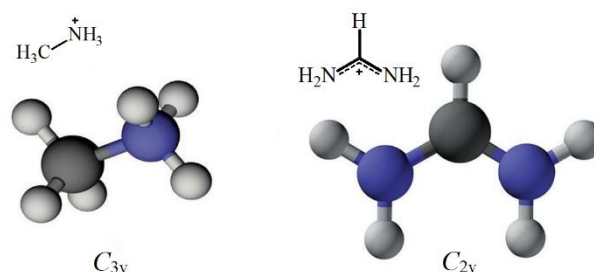


Fig. 1. Structure of the isolated  $\text{MA}^+$  and  $\text{FA}^+$  ions with the designated point group

### 3.1. IR band analysis

In the absorption spectra of both MAI and FAI, a broad band at  $3400\text{ cm}^{-1}$  can be observed, as well as a band at  $1640\text{ cm}^{-1}$ . These bands will not be considered since it is obvious that they arise from the water molecules present in the liquid nitrogen cell at the beginning of the recordings. As the heating of the cell starts, these bands diminished and once they are gone upon cooling they do not reappear.

In Figures 2 and 3 the IR spectra of MAI and FAI representing each phase (according to the provided scheme) are given. The assignation is done

according to the transmittance spectra. The reflectance (ATR) spectra are only used to confirm the assignment in the moderate and high-temperature

phases since the ATR spectra are recorded starting from room temperature up to +200 °C.

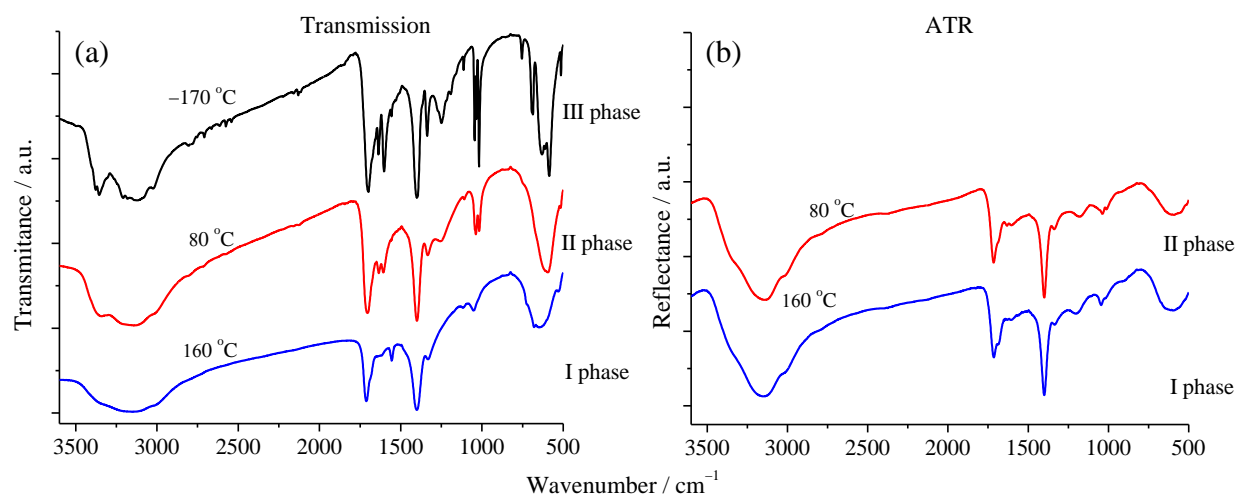


**Fig. 2.** (a) Transmission and (b) ATR spectra of MAI showing the low temperature phase –  $\beta'$ , moderate temperature phase –  $\alpha$ , and high temperature phase –  $\epsilon$ . For clarity, the spectra are separated along the y-axis, so the transmittance and reflectance are given in arbitrary unites.

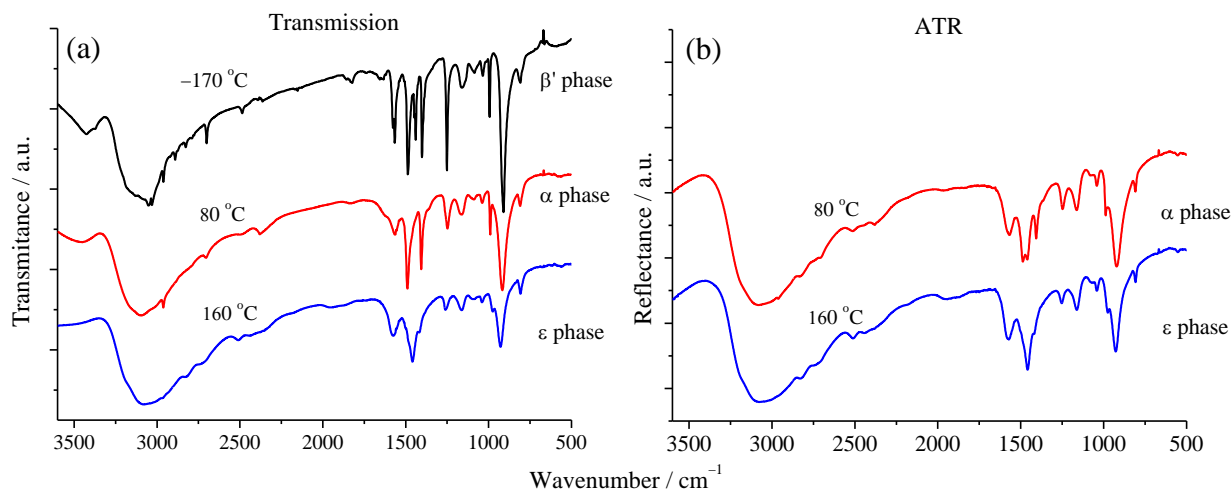


**Fig. 3.** (a) Transmission and (b) ATR spectra of FAI showing the lower temperature phase – III, and high temperature phases – II and I, respectively. For clarity, the spectra are separated along the y-axis, so the transmittance and reflectance are given in arbitrary unites.

### 3.1.1. Region of stretching vibrations

In this spectral region bands arising from the symmetric and asymmetric vibrations of the  $\text{CH}_3$  and  $\text{NH}_3^+$  groups present in  $\text{MA}^+$  could be found. In the high frequency end of the FAI spectra, where most of the combinational modes are pre-

sent, the bands from the  $\text{NH}_2$  groups are observed. The partial and full deuteration on MAI [7] suggests that the region above  $3030\text{ cm}^{-1}$  does not have bands from the  $\text{CH}_3$  group vibrations. This fact led to problematic suggestions in the assignation made in [6].

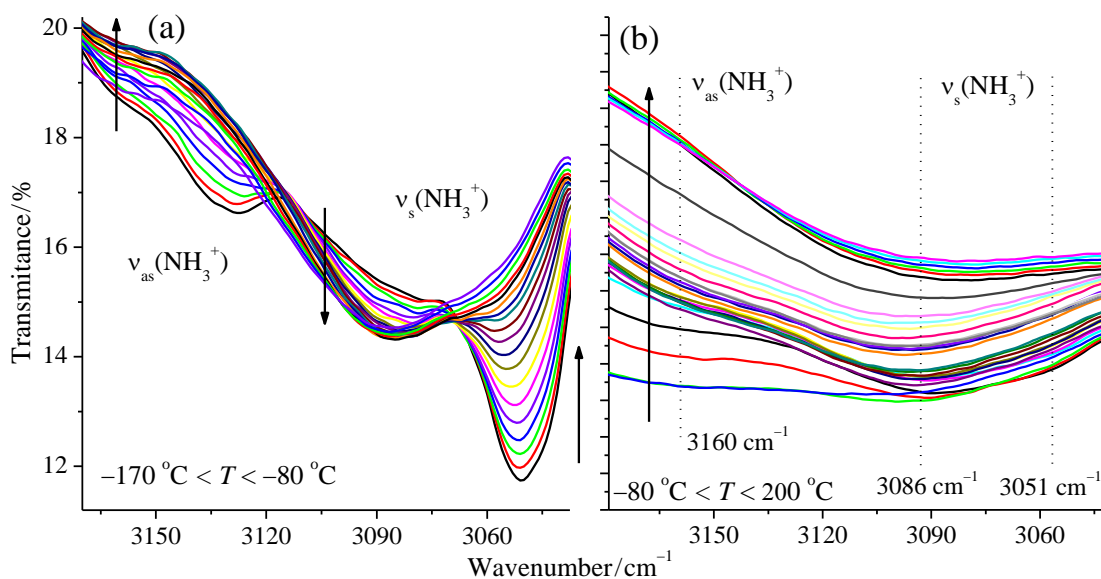


**Fig. 4.** The infrared transmission spectra of MAI in the temperature range (a) from  $-170$  to  $-80$  °C and (b) from  $-75$  to  $200$  °C. The temperature differences between the spectra are five degrees in the range from  $-170$  to  $-60$  °C and in the range from  $-60$  to  $200$  °C, the difference is  $10$  °C. The arrows indicate the direction of the temperature increase.

The development of the  $\nu_{as}(\text{NH}_3^+)$  and  $\nu_s(\text{NH}_3^+)$  in the entire temperature range is given in Figure 4. According to the spectra in this figure, it can be concluded that the band at  $3050\text{ cm}^{-1}$  from the symmetric  $\text{NH}_3^+$  stretching vibrations diminishes as the temperature increases. On the other hand, the band at  $3090\text{ cm}^{-1}$  appears, as the band at  $3050\text{ cm}^{-1}$  diminishes. These two bands are inter-

connected with an isosbestic point that appears at around  $3068\text{ cm}^{-1}$  and indicates the reorientation of the  $\text{NH}_3^+$  groups in the crystal structure as the temperature rises. It is obvious that these two bands do not disappear but they fuse together with the bands from the combinational vibrations in the vicinity ( $3030\text{ cm}^{-1}$ ). So for the  $\beta'$  and  $\alpha$  phase of MAI the wavenumbers for the  $\nu_{as}(\text{NH}_3^+)$  and  $\nu_s(\text{NH}_3^+)$  are:

$\text{NH}_3^+$	$\beta'$ ( $-170$ to $-110$ °C)	$\alpha$ ( $-110$ to $146$ °C)	$\epsilon$ ( $146$ to $200$ °C)
	3161 to 3164; at $-150$ °C merges with the combinational band $\delta_{as}(\text{NH}_3^+) + \delta_s(\text{NH}_3^+)$		
$\nu_{as}/\text{cm}^{-1}$	3134 to 3133 ( $-140$ °C)		
	3128 to 3133 ( $-140$ °C)	above $-140$ °C merges to 3082	
	3086 to 3082	3082 to 3066 ( $-40$ °C)	
$\nu_s/\text{cm}^{-1}$	3051 to 3057	3057 to 3066 ( $-40$ °C)	3066 to 3083

(The values in the brackets indicate the temperature at which the band disappears in the adequate phase)

According to the findings in Cabana et al. [5], the band at  $3050\text{ cm}^{-1}$  from the low-temperature phase is assigned as  $\nu_s(\text{NH}_3^+)$  mode and for the room temperature phase this band shifts to  $3012\text{ cm}^{-1}$ . According to Fig. 4a, this assignment can be considered as incorrect since it is obvious that the band shifts to higher values for the wavenumber for the room temperature phase.

The stretching vibrations of the  $\text{CH}_3$  groups give bands at  $2962$  and  $2919\text{ cm}^{-1}$  for the asymmetric and symmetric mode, respectively. Even though the band at  $2962\text{ cm}^{-1}$  diminishes drastically, its presence in the spectra at  $200$  °C can still be observed. Unlike the asymmetric vibration, the band from the symmetric vibration disappears at around  $-65$  °C. The wavenumbers of these bands are:

$\text{CH}_3$	$\beta'$ ( $-170$ to $-110$ °C)	$\alpha$ ( $-110$ to $146$ °C)	$\epsilon$ ( $146$ to $200$ °C)
$\nu_{as}/\text{cm}^{-1}$	2962	2962	2962 to 2967
$\nu_s/\text{cm}^{-1}$	2920	2920 ( $-65$ °C)	

The stretching vibrations of the NH<sub>2</sub> groups in the FAI are located in the frequency region from 3400 to 3000 cm<sup>-1</sup>. The origin of these bands can be additionally confirmed by the IR spectra obtained from the chloroformamidinium chloride

[ClC(NH<sub>2</sub>)<sub>2</sub>]Cl [22]. In the low-temperature region, the number of bands is higher, but as the temperature increases, the bands shift and they merge into one band (Fig. 5). The wavenumbers of these bands, corresponding to the certain phase are:

NH <sub>2</sub>	III (-170 to 73 °C)	II (73 to 115 °C)	I (115 to 200 °C)
	3377 to 3373 (35 °C)		
$\nu_{as}/\text{cm}^{-1}$	3355 to 3347	3347 to 3345	
	3305 to 3309		
	3281		merged to very broad band
	3208		3500 – 2800 cm <sup>-1</sup>
$\nu_s/\text{cm}^{-1}$	3180	merged to very broad band	
	3140	3290 – 2900 cm <sup>-1</sup>	
	3118		

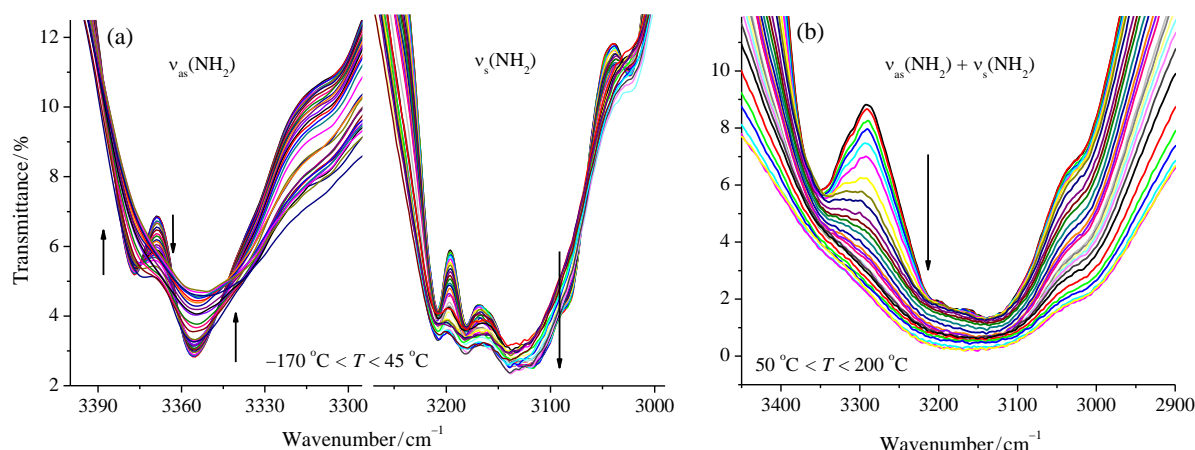


**Fig. 5.** Temperature dependent spectra of FAI in the region of stretching vibrations recorded in the temperature interval from (a) -170 to 45 °C and (b) from 50 to 200 °C. The arrows indicate the direction of the temperature increase.

In FAI, the carbon atom is bonded to a single hydrogen atom, and the C–H stretching vibrations of this group will give band in the region from 3000 to 2750 cm<sup>-1</sup>. In the recorded spectra, these bands diminish as the temperature increases.

At high temperatures, they have very weak intensity, and the band at 3000 cm<sup>-1</sup> merges with the one from the NH<sub>2</sub> vibrations forming a wider band. The assignment in the entire temperature range is given:

C–H	III (-170 to 73 °C)	II (73 to 115 °C)	I (115 to 200 °C)
	3024 to 3016	3016 to 3015	3015 to 3010 (sh) vw
$\nu/\text{cm}^{-1}$	2915		
	2806 to 2807	2807 to 2813	2813 to 2795 vw

### 3.1.2. Deformation vibrations

In this section, the in-plane bending vibrations of the NH<sub>3</sub><sup>+</sup>, NH<sub>2</sub> and CH<sub>3</sub> groups will be considered followed by the analysis of the rocking, wagging and twisting modes. The out-of-plane CH vibrations of the FAI will also be considered here even though they are with combinational origin at higher temperatures.

### In-plane bending vibrations

The asymmetric (Fig. 6a) and symmetric (Fig. 6b) bending vibrations of NH<sub>3</sub><sup>+</sup> groups in MAI give bands in the region from 1580 to 1470 cm<sup>-1</sup>. In Figure 6 all spectra in the temperature range from -170 to 200 °C are shown. The temperature difference between the spectra in the low-



temperature region are 5 degrees and in the region between  $-30$  and  $200$  °C, the differences are 10 degrees. Additionally, the spectra recorded in the vicinity of the transition temperature ( $146$  °C) are also given. It is obvious that as the temperature increases, the bands originating from the asymmetric bending deformation merge into one broad band. On the other hand, the band assigned to the symmetric bending vibrations vanishes when MAI undergoes the  $\alpha \rightarrow \epsilon$  phase transition.

The band shape of the  $\delta_s(\text{NH}_3^+)$  vibrations in the low-temperature range (at  $1487$   $\text{cm}^{-1}$  for  $-170$  °C), suggests presence of two bands as found for the MAI [12]. In the case of MAI this splitting at low temperatures ( $-170$  °C) is not as pronounced as in the case of MAI, although the temperature of the recorded MAI spectra is stated to be  $-185$  °C. The change in the position and the disappearance of the bands from the bending  $\text{NH}_3^+$  groups is summarized:

$\text{NH}_3^+$	$\beta'$ ( $-170$ to $-110$ °C)	$\alpha$ ( $-110$ to $146$ °C)	$\epsilon$ ( $146$ to $200$ °C)
$\delta_{\text{as}}/\text{cm}^{-1}$	1577 to 1573 (sh)	1573 to 1572 ( $-70$ °C)	
	1566 to 1565	1565 to 1569 (vb)	1569 to 1575
$\delta_s/\text{cm}^{-1}$	1487 to 1488	1488 to 1486	1486 to 1484 (sh)

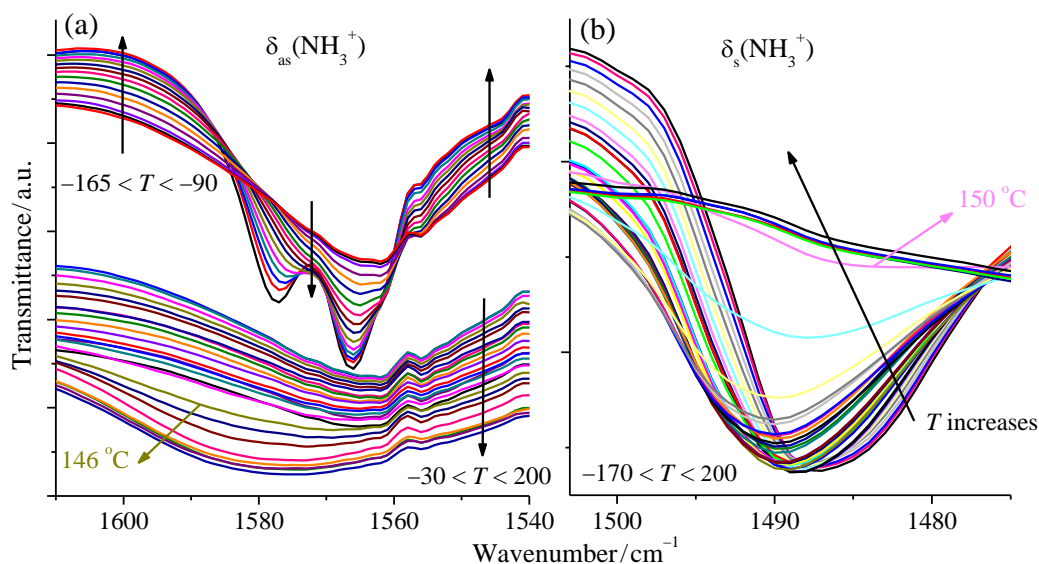


**Fig. 6.** IR spectra of MAI. (a) Asymmetric  $\text{NH}_3^+$  bending vibrations in the range between  $-165$  and  $-90$  °C (upper set) and between  $-30$  and  $200$  °C (lower set of spectra). (b) Symmetric  $\text{NH}_3^+$  bending vibrations in the entire temperature interval ( $-165$  to  $200$  °C).

The important band assembly is the one formed by the asymmetric bending  $\text{CH}_3$  vibrations. Its importance is in the fact that these bands are part of an isosbestic point formation that can reveal the exact temperature at which the phase transition occurs [17]. Additionally, they show the appear-

ance/disappearance of the bands so their evolution and assignment can be followed only by investigating the temperature dependent spectra. The entire temperature region of this spectral range is presented in Figure 7, so the assignment can be made with high degree of certainty:

$\text{CH}_3$	$\beta'$ ( $-170$ to $-110$ °C)	$\alpha$ ( $-110$ to $146$ °C)	$\epsilon$ ( $146$ to $200$ °C)
	1457	1461 to 1460	1460 to 1459
$\delta_{\text{as}}/\text{cm}^{-1}$	1447 to 1444	1453 to 1454	1454
	1440 to 1444	1444 to 1446 ( $-70$ °C)	
	1402	1402 to 1407	1407 to 1418 (w)
$\delta_s/\text{cm}^{-1}$	1394 ( $-125$ °C)		
	1385	1385 ( $5$ °C)	

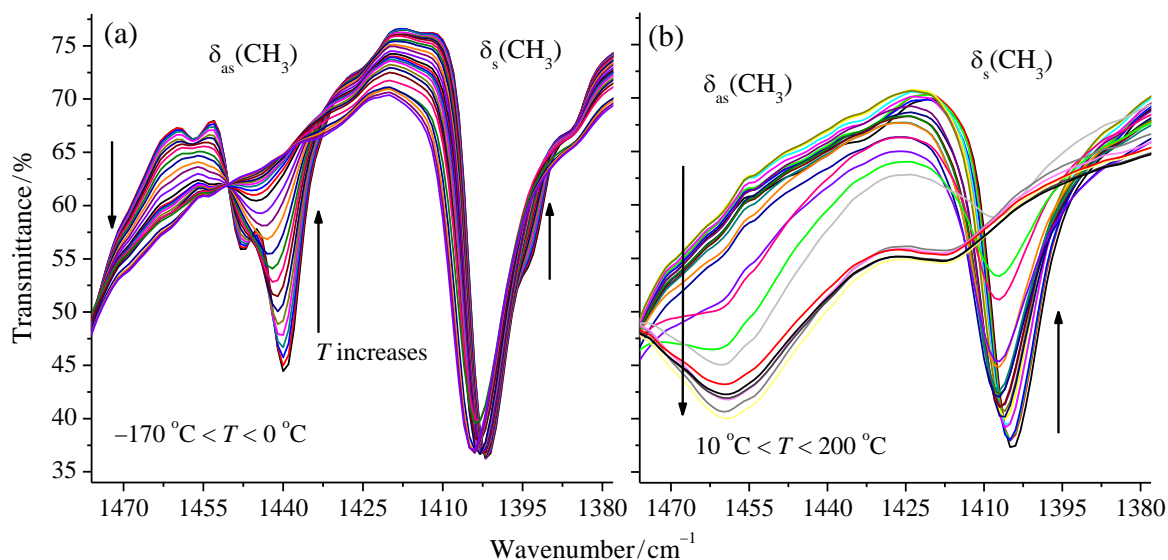


**Fig. 7.** Region of bending CH<sub>3</sub> group vibrations in MAI. The bands from the CH<sub>3</sub> groups are associated with the isosbestic points occurring for both phase transitions (a) in the low-temperature region (around  $-110\text{ }^{\circ}\text{C}$ ) and (b) in the temperature region around  $146\text{ }^{\circ}\text{C}$  where the second phase transition occurs. The arrows indicate the direction of the temperature increase.

The bands arising from the NH<sub>2</sub> bending vibrations in FAI are not as clearly distinguished as the ones from the NH<sub>3</sub><sup>+</sup> groups in MAI. Most of these bands are with combinational origin. A proof for that can be found in the DFT calculations [19].

According to the spectra shown in Figure 8, the shape of the band appearing at  $1602\text{ cm}^{-1}$  suggests presence of a doublet. The wavenumbers of the bending vibrations of NH<sub>2</sub> groups for all three phases are assigned as:

NH <sub>2</sub>	III ( $-170$ to $73\text{ }^{\circ}\text{C}$ )	II ( $73$ to $115\text{ }^{\circ}\text{C}$ )	I ( $115$ to $200\text{ }^{\circ}\text{C}$ )
$\delta/\text{cm}^{-1}$	1637 to 1635	1635 to 1634	1634 to 1638 ( $140\text{ }^{\circ}\text{C}$ )
	1602 to 1606	1606 to 1616	1616 to 1618 (vw)

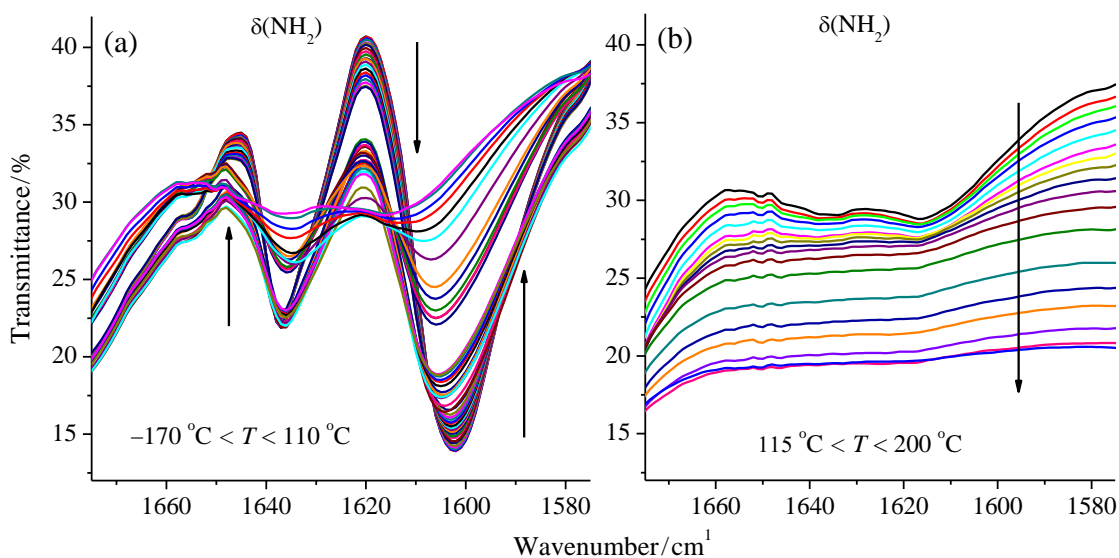


**Fig. 8.** Region of bending NH<sub>2</sub> group vibrations in FAI. Spectra recorded (a) between  $-170$  and  $110\text{ }^{\circ}\text{C}$  and (b) up to  $200\text{ }^{\circ}\text{C}$ . The arrows indicate the direction of the temperature increase.



### Rocking, wagging and twisting vibrations

The bands originating from these vibrations are below  $1350\text{ cm}^{-1}$  and are present in both MAI and FAI spectra for the  $\text{NH}_3^+$ ,  $\text{CH}_3$  and  $\text{NH}_2$  groups. They are usually combinations (between each other), but at a certain extent, they can be present as pure rocking, wagging and twisting vibrations especially in the low-temperature region.

In the case of MAI, only the rocking mode of  $\text{NH}_3^+$  and  $\text{CH}_3$  can be observed in the IR spectra. According to the presented spectra in Figure 9, one can conclude that there is not only a band shift, but there is also a change in the intensity of

the bands. It is interesting to mention that the band from the rocking  $\text{NH}_3^+$  vibrations has a change in the intensity right at the phase transition temperature [17,23], as can be observed in the spectra in Figure 9b. It is important to study the changes that occur in narrower temperature intervals in order not to be misled. If one analyzes Figure 9a only, it might look like that there are two bands that form while increasing the temperature. However, if the analysis includes the spectra given in Figure 9b (one degree temperature difference of recorded spectra), a more precise conclusion can be made. Namely, it is clearly visible that only a band shift occurs (Fig. 9b). The band positions are given as:

$\text{NH}_3^+$ ; $\text{CH}_3$	$\beta'$ ( $-170$ to $-110\text{ }^\circ\text{C}$ )	$\alpha$ ( $-110$ to $146\text{ }^\circ\text{C}$ )	$\varepsilon$ ( $146$ to $200\text{ }^\circ\text{C}$ )
$\rho(\text{NH}_3^+)/\text{cm}^{-1}$	1251 to 1250	1250 to 1259	1259 to 1261
$\rho(\text{CH}_3)/\text{cm}^{-1}$	918 to 920	920 to 920 ( $-90\text{ }^\circ\text{C}$ )	
	910 to 911	911 to 923	923 to 930

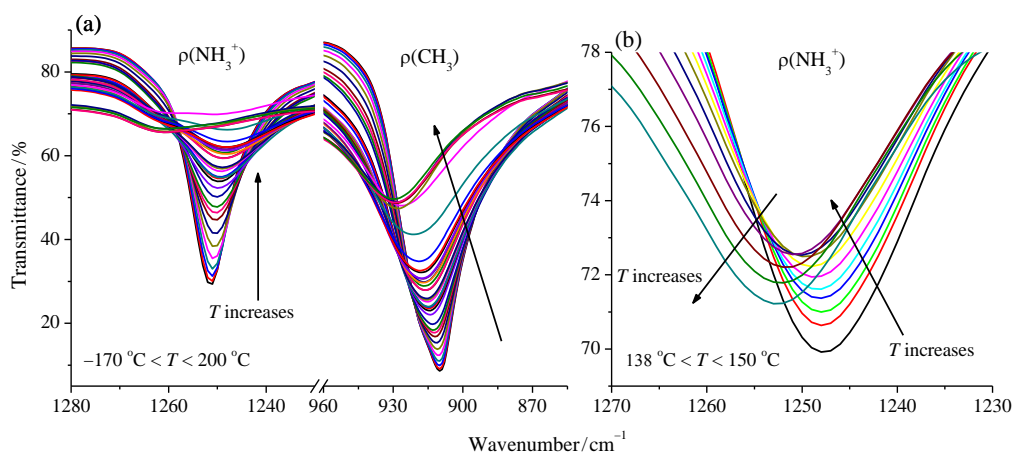


**Fig. 9.** Spectra representing the regions of rocking vibrations of  $\text{NH}_3^+$  and  $\text{CH}_3$  groups in MAI. The recorded spectra are with (a) ten degree difference in the region from  $-170$  to  $200\text{ }^\circ\text{C}$  and (b) one degree difference in the region from  $138$  to  $150\text{ }^\circ\text{C}$ .

In the case of FAI, there are three bands originating from the rocking  $\text{NH}_2$  vibration and the other deformation vibrations are assigned to the wagging and twisting modes. One of the rocking modes tends to merge with the other bands originating from the  $\text{CH}$  deformation vibrations, so it will be considered in the section “combinational bands” (Fig. 14). The other  $\rho(\text{NH}_2)$  vibrational modes are

relatively simple and with predictable behavior so they will not be considered in more details.

By the spectra presented in Figure 10, it is obvious that at higher temperatures the bands from the twisting and wagging modes fuse into a single broad band. This is observed in the low-frequency region (Fig. 10b). The changes in band positions regarding the values for the wavenumbers are:

$\text{NH}_2$	III ( $-170$ to $73\text{ }^\circ\text{C}$ )	II ( $73$ to $115\text{ }^\circ\text{C}$ )	I ( $115$ to $200\text{ }^\circ\text{C}$ )
	1273 to 1269 ( $-80\text{ }^\circ\text{C}$ )		
$\rho/\text{cm}^{-1}$	1249 to 1254 1045 to 1044	1254 to 1249 ( $90\text{ }^\circ\text{C}$ ) 1044 ( $80\text{ }^\circ\text{C}$ ), merged with $\delta(\text{CH})$ , see Fig. 14	
	1113 to 1110	1110 to 1112	1112 to 1119 ( $170\text{ }^\circ\text{C}$ )
$\tau/\text{cm}^{-1}$	514 to 516 687 to 665 631 to 620	516 to 521 merges with $\gamma(\text{CH})$ at $-80\text{ }^\circ\text{C}$ , 683 (see Fig. 11) 620	521 merged to 622
$\omega/\text{cm}^{-1}$	612 586 to 592	612 592 to 596 ( $80\text{ }^\circ\text{C}$ )	merged to 622

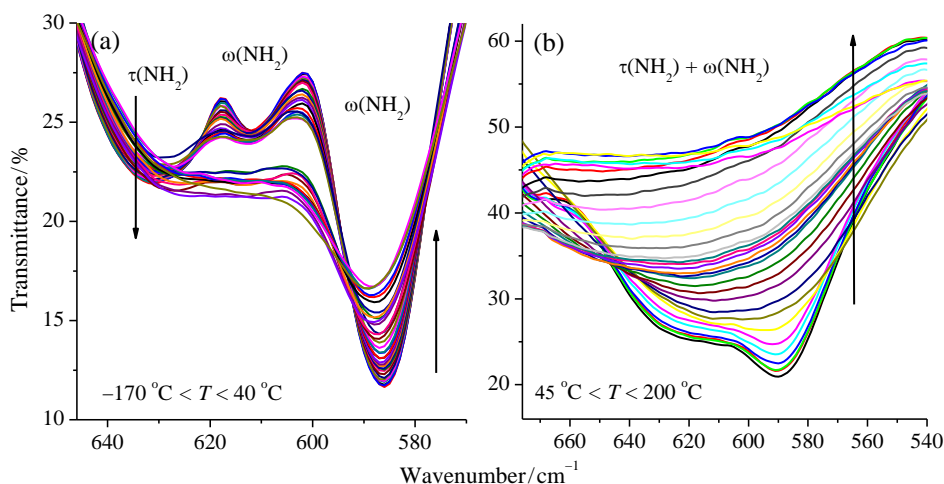


**Fig. 10.** Region of the rocking, wagging and twisting vibrations in FAI for the (a) low-temperature range and (b) high-temperature range. The bands tend to fuse together as the temperature increases.

### Out-of-plane vibrations

The assignment of the out-of-plane CH vibration in FAI has been previously reported [11, 19] but has not been addressed properly since it is more difficult to distinguish the band origin at room temperature rather than at the liquid N<sub>2</sub> temperatures. From our detailed analysis of the bands given in Figure 11, several conclusions can be drawn. First, the band at 693 cm<sup>-1</sup> fuses together with the one at 687 cm<sup>-1</sup> at -80 °C, forming a new band at 686 cm<sup>-1</sup>. The obtained new band behaves similarly as the one at 754 cm<sup>-1</sup> assigned as  $\gamma(\text{CH}) + \tau(\text{NH}_2)$  [11]. This result leads to the conclusion

regarding the assignment of the starting bands (693 cm<sup>-1</sup> and 687 cm<sup>-1</sup>). More precisely, the band at 693 cm<sup>-1</sup> is assigned as  $\gamma(\text{CH})$  and the one at 687 cm<sup>-1</sup> as  $\tau(\text{NH}_2)$ . Above -80 °C the combined band (now at 680 cm<sup>-1</sup>) shifts towards lower values for the wavenumber until it merges with another combinational band  $\tau(\text{NH}_2) + \omega(\text{NH}_2)$ . The formation of the later band is shown in Figure 11b. It is interesting that both bands (680 and 754 cm<sup>-1</sup>) disappear above 75 °C, and then reappear at 115 °C when the phase transition takes place [17].

These new findings enable more precise assignment of the bands appearing in the low-frequency region.

CH	III (-170 to 73 °C)	II (73 to 115 °C)	I (115 to 200 °C)
$\tau(\text{NH}_2) + \gamma(\text{CH})/\text{cm}^{-1}$	754 to 750	disappears	727 to 728
$\gamma(\text{CH})/\text{cm}^{-1}$	693 merges with $\tau(\text{NH}_2)$ at -80 °C, to 684		reappears at 115 °C, 680

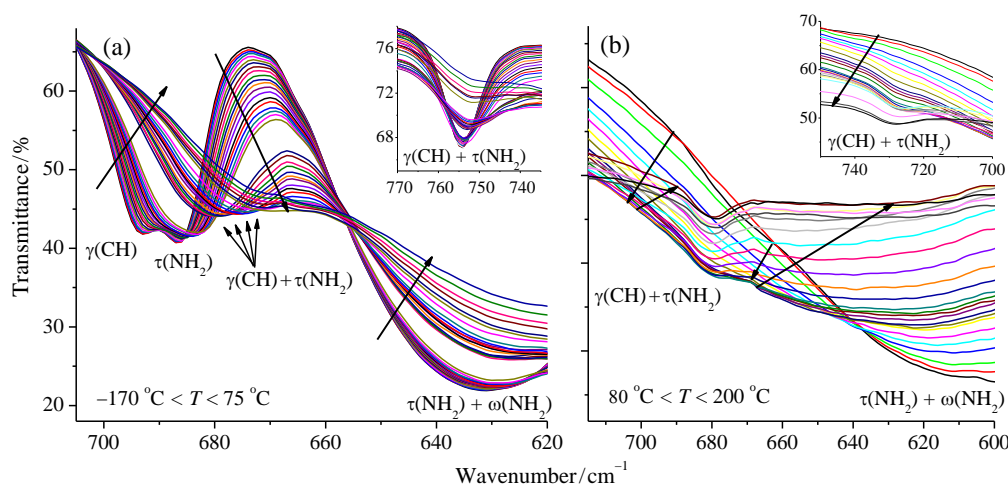


**Fig. 11.** Region of the out-of-plane CH vibrations and NH<sub>2</sub> twisting vibrations as a function of temperature in FAI. Both insets depict the behavior of the higher frequency  $\gamma(\text{CH})$  band. The spectra are recorded (a) from -170 to 75 °C and (b) up to 200 °C.

### 3.1.3. Skeletal vibration

Characteristic feature in the IR spectra of both MAI and FAI are the bands arising from the C–N stretching vibrations. The phase transition in

MAI is due to the changes of the CH<sub>3</sub> and NH<sub>3</sub><sup>+</sup> rotations against the C<sub>3</sub> axis over the C–N bond, which is observed in the spectra. In the MAI spectra, the  $\nu(\text{C–N})$  appears at around 990 cm<sup>-1</sup>:

MAI	$\beta'$ (–170 to –110 °C)	$\alpha$ (–110 to 146 °C)	$\epsilon$ (146 to 200 °C)
$\nu/\text{cm}^{-1}$	994 to 993	993 to 988	988 to 974

The "purity" of the bands assigned to the C–N vibrations in the FAI is questionable. It is apparent that the band at 1700 cm<sup>-1</sup> consists of several bands and at low temperatures two maxima can be distinguished (Fig. 12a). This enables to understand the bands' nature. Accordingly, this complex band can be assigned as combinational band, even though the highest contribution is by N–C–N vibration [11, 19]. The assignation of this complex band is possible because of the opportunity to follow its evolution as a function of temperature. In

the low-temperature region, the assignation can be made as shown in Figure 12a. Unexpectedly, the bands at higher temperatures are more pronounced and more distinguishable (Fig. 12b). This could be a consequence of the symmetry of the FA<sup>+</sup>. At low-temperatures the rigidity of the NH<sub>2</sub> groups is higher. Because of that the NH<sub>2</sub> motion is more restricted. On the other hand, the increase in temperature results in more pronounced NH<sub>2</sub> activity that disturbs the symmetry. The wavenumber of the peaks could be summarized as:

FAI	III (–170 to 73 °C)	II (73 to 115 °C)	I (115 to 200 °C)
$\nu_{\text{as}}(\text{NCN})/\text{cm}^{-1}$	1704 to 1708	1708 to 1711	1711 to 1710
$\delta(\text{CH})/\text{cm}^{-1}$	1698 to 1699	1699 to 1703	1703 to 1701
$\delta(\text{NH}_2)/\text{cm}^{-1}$	1687 to 1687	1687 to 1686	1686 to 1685
	1676 to 1676	1676 to 1678	1678 to 1679
$\nu_{\text{s}}(\text{NCN})/\text{cm}^{-1}$	1400	1400	1400
	1364		
$\nu_{\text{s}}(\text{NCN})/\text{cm}^{-1}$	1337 to 1335	1334 to 1332	1332 to 1333 vw

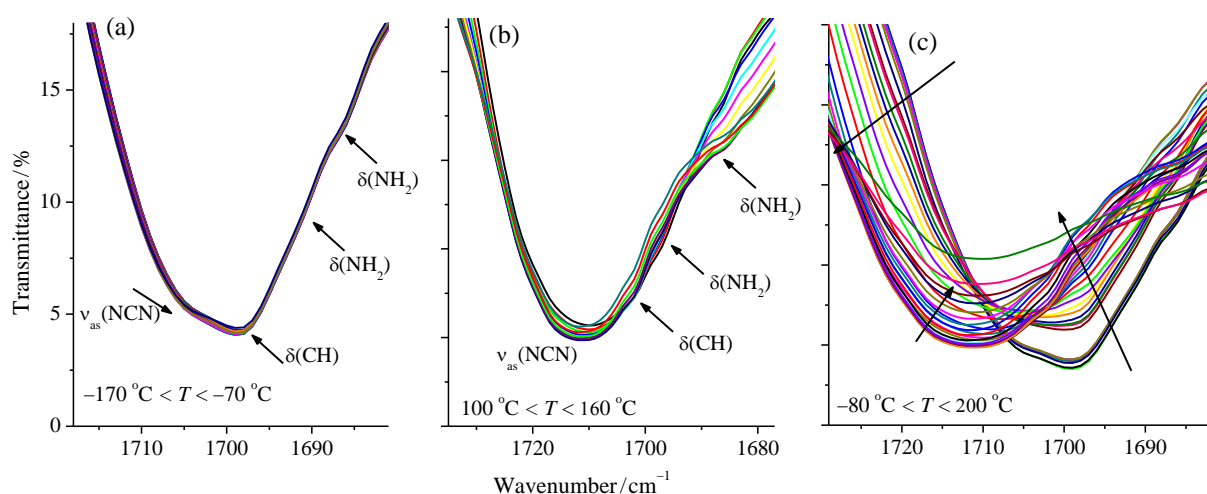


**Fig. 12.** Combinational band  $\nu_{\text{as}}(\text{NCN}) + \delta(\text{CH}) + \delta(\text{NH}_2)$  in FAI for the temperature range (a) from –170 to –70 °C, (b) from 100 to 160 °C and (c) the transition between the two clearly distinguished states.

Even though the entire band assembly is a complex combinational band, as a result of the fact that the major contribution to the band intensity is

by the stretching C–N vibration, it is considered in this section.

### 3.1.4. Overtones and combinations

In this section, the overtones and the combination vibrations of MAI will be considered. In the case of FAI, no overtones were observed in the vibrational spectra. Part of the combination vibrations in FAI were studied in the section regarding the bands arising from the deformation vibrations ( $\gamma(\text{CH}) + \tau(\text{NH}_2)$ ). This is a consequence of their origin and the fact that they consist of pure vibra-

tional modes in the low-temperature range. The rest of the combinational modes are considered at the end of this section.

Four bands in the spectra of MAI are assigned as overtones. Some are present only in the low-temperature range and understandably, all of them are with low intensity. For the  $\epsilon$  phase most of the bands disappear except the overtone from the  $\delta_s(\text{CH}_3)$ . The assignment is as follows:

$\text{NH}_3^+; \text{CH}_3$	$\beta'$ (–170 to –110 °C)	$\alpha$ (–110 to 146 °C)	$\epsilon$ (146 to 200 °C)
$2\delta_{\text{as}}(\text{NH}_3^+)/\text{cm}^{-1}$	3218 vw		
$2\delta_{\text{as}}(\text{CH}_3)/\text{cm}^{-1}$	2890 to 2896	2896 to 2901 (65 °C)	
	2875 to 2882	2882 to 2887 (120 °C)	
$2\delta_s(\text{CH}_3)/\text{cm}^{-1}$	2789 to 2791		
	2776 to 2779	2779 to 2830	2830 to 2837
	1833 to 1829		
$2\rho(\text{CH}_3)/\text{cm}^{-1}$	1831 to 1829	1829 (merged at –70 °C)	1845 to 1887
	1823 to 1824		

The overtones worth mentioning are the ones from the  $\text{CH}_3$  bending vibrations  $\delta(\text{CH}_3)$ . Both the asymmetric and symmetric fundamental stretching vibrations are part of an isosbestic point

(Fig. 7). If the bands from the overtones of these vibrations are considered (Fig. 13), another set of isosbestic points can be observed. This finding supports the assignment of the overtones.

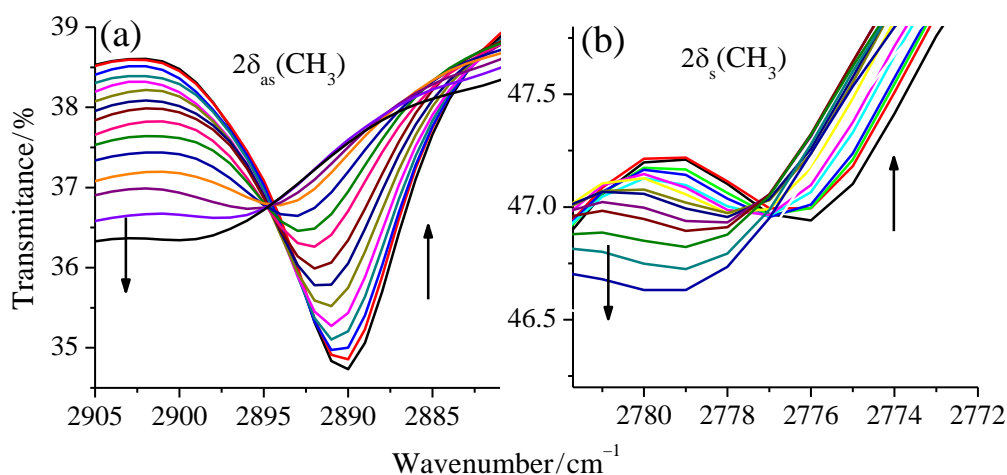


**Fig. 13.** Overtones of the  $\text{CH}_3$  bending vibrations in MAI are part of an isosbestic point formation, finding that confirms the proper assignment not only of the overtones, but also of the fundamental vibrational modes. The presented spectra are recorded in the temperature range from –170 to –110 °C.

The most complex band assembly is the one in the region of stretching  $\text{NH}_3^+$  vibrations. These bands are in their pure state only at very low temperatures. As the temperature is increased, the

complexity is even more pronounced and is harder to assign them unambiguously. The proposed assignment is as follows:

MAI / $\text{cm}^{-1}$	$\beta'$ (–170 to –110 °C)	$\alpha$ (–110 to 146 °C)	$\epsilon$ (146 to 200 °C)
$\delta_{\text{as}}(\text{NH}_3^+) + \delta_{\text{s}}(\text{NH}_3^+)$	3187; at –150 °C merges with $\nu_{\text{as}}(\text{NH}_3^+)$		
$\delta_{\text{as}}(\text{NH}_3^+) + \delta_{\text{s}}(\text{NH}_3^+), \nu_{\text{as}}(\text{NH}_3^+)$	3168 to 3158	3158 to 3180	3180 to 3188
$\delta_{\text{as}}(\text{NH}_3^+) + \delta_{\text{as}}(\text{CH}_3)$	3030 to 3031	3031 to 3036	3036 to 3036
$\delta_{\text{s}}(\text{NH}_3^+) + \delta_{\text{as}}(\text{CH}_3)$	2995		
$\delta_{\text{s}}(\text{CH}) + \delta_{\text{as}}(\text{CH}_3)$	2850 to 2852 2828 to 2839	2852 to 2858	
$\delta_{\text{as}}(\text{CH}_3) + \rho(\text{NH}_3^+)$	2701 to 2702	2702 to 2708	2708 to 2731
$\delta_{\text{as}}(\text{NH}_3^+) + \rho(\text{CH}_3)$	2486 to 2487	2487 to 2510	2510 to 2512
$\delta_{\text{s}}(\text{NH}_3^+) + \nu(\text{CN})$	2447 to 2446	2446 to 2449	2449 to 2445
$\delta_{\text{as}}(\text{CH}_3) + \rho(\text{CH}_3)$	2391 to 2387 2377 to 2378 2363 to 2365 2353 to 2351 2347 to 2344	2387 to 2388 (–50 °C) 2378 to 2381 2365 to 2368 2351 to 2357 2344 to 2343	2381 to 2382  2357 to 2362
$\rho(\text{NH}_3^+) + \rho(\text{CH}_3)$	2166 to 2170 2152 to 2152 2131 to 2137	2170 2152 2137	2177 to 2177
$\nu(\text{CN}) + \rho(\text{CH}_3)$	1868 to 1868 1858 to 1859		1951 to 1954

The last combinational band to be considered is the one originating from the deformation vibrations in FAI. In the low temperature region a distinct band shapes could be observed, so the assignment is relatively simple. On the other hand, as the temperature increases, the band structure becomes more complex. In Figure 14a the spectra in the temperature range corresponding to the phase III (from –170 to 65 °C) are shown. It is obvious

that the bands assigned as  $\rho(\text{NH}_2)$  and  $\delta(\text{CH})$  start to fuse together, but at the point of the phase transition (Fig. 14b), the fused band continues to “develop” independently. At the next phase transition, this band starts to shift towards higher wavenumber values. At higher temperatures (Fig. 14c) all three bands in question fuse together. The changes in the wavenumber are:

FAI	III (–170 to 73 °C)	II (73 to 115 °C)	I (115 to 200 °C)
$\rho(\text{NH}_2)/\text{cm}^{-1}$	1045 to 1044	1037 to 1048	1048 to 1056
$\delta(\text{CH})/\text{cm}^{-1}$	1034 to 1037		
$\gamma(\text{CH})/\text{cm}^{-1}$	1018 to 1017	1017.4 to 1023	1023 to 1046

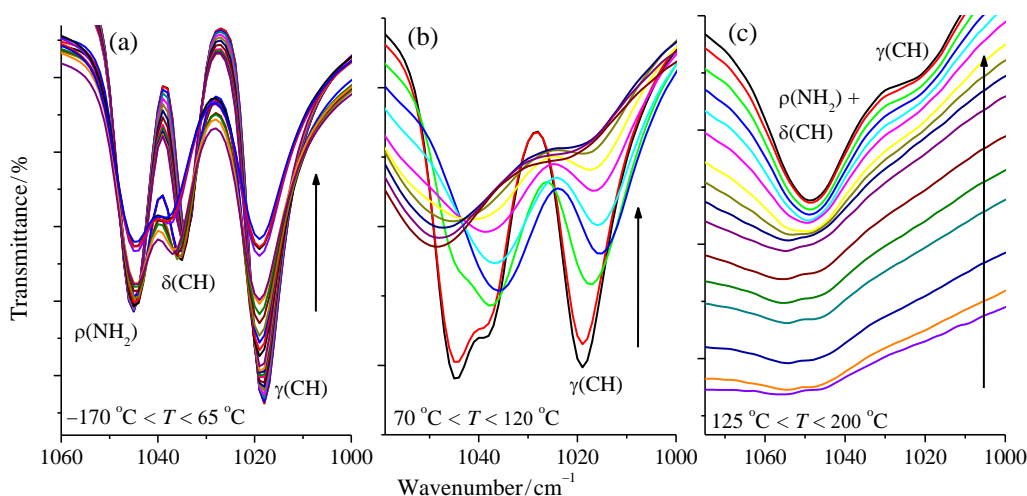


**Fig. 14.** Combinational band  $\rho(\text{NH}_2) + \delta(\text{CH}) + \gamma(\text{CH})$  in FAI that is obtained by the increase in temperature. Behavior of the bands in the temperature range (a) before the first phase transition (from –170 to 65 °C), (b) around the first and second transition, (c) after the second transition (above 125 °C).

The results obtained by the analysis of the temperature dependent IR and ATR spectra for all stable phases of MAI and FAI are summarized in Table S1 and S2 given in the Supplementary material.

### 3.2. Raman spectra

Raman spectra (Fig. S1) reveal the characteristic features of MAI  $\alpha$  phase and phase I of

FAI. The Raman shift for the bands of MAI and FAI are given in Table 1. These spectra are relatively simpler compared to the infrared spectra of the same compounds.

The assignment of the bands in the Raman spectra is made according to the available literature data [6, 9, 19, 24–27]. These results assisted the assignment of the bands in the IR spectra, the once involved in the phase transition as well as the characterization of the change during the phase transition.

Table 1

Raman shift for the room temperature phases of MAI and FAI

MAI			FAI		
$\tilde{\nu}/\text{cm}^{-1}$	Assignment	Acc. to ref.	$\tilde{\nu}/\text{cm}^{-1}$	Assignment	Acc. to ref.
			3360 s		
			3254 m		
			3192 s	$\nu(\text{NH}_2)$	[24]
			3142 m		
3127	$\nu_{\text{as}}(\text{NH}_3^+)$	[25]			
3079 s	$\nu_{\text{s}}(\text{NH}_3^+)$	[25]			
2958 m	$\nu_{\text{as}}(\text{CH}_3)$	[25]			
2899 m			3083 m		
2883 m	$\nu_{\text{s}}(\text{CH}_3)$	[25]	3025 w	$\nu(\text{CH})$	[9, 24]
			1697 vw	$\nu_{\text{as}}(\text{NCN})$	[24]
1608 b	$\delta_{\text{as}}(\text{NH}_3^+)$	[6, 25, 26]	1608 b	$\delta(\text{NH}_2)$	[24]
1533 s	$\delta_{\text{s}}(\text{NH}_3^+)$	[6, 25, 26]			
1456 m	$\delta_{\text{as}}(\text{CH}_3)$	[6, 25, 26]	1551 w		
1401 w	$\delta_{\text{s}}(\text{CH}_3)$	[6]	1527 w	$\delta(\text{CH})$	[9, 24]
			1372 s	$\delta(\text{CH}) + \nu_{\text{as}}(\text{NCN})$	[9, 19]
			1333 m	$\rho(\text{NH}_2)$	[9, 19]
985 m	$\nu(\text{CN})$	[6, 27]	1109 m	$\nu_{\text{s}}(\text{NCN})$	[9, 19]
			1036 w	$\rho(\text{NH}_2) + \gamma(\text{CH})$	[9, 19]
907 m	$\rho(\text{CH}_3)$	[6]	1017 w	$\rho(\text{NH}_2)$	
			740 w	$\tau(\text{NH}_2) + \gamma(\text{CH})$	[19]
			677 m	$\omega(\text{NH}_2)$	[9]
			627 sh	$\delta(\text{CN})$	[19]
			607 w	$\tau(\text{NH}_2)$	[9, 19]
			512 m	$\delta(\text{CN})$	[19]
108 m	$\text{T}(\text{MA}^+)$	[6]	142 s	$\text{T}(\text{FA}^+)$	[19]
			116 s	$\text{L}(\text{FA}^+)$	[19]

## 4. CONCLUSION

For the first time the vibrational spectra of MAI and FAI in wide temperature range ( $-170$  °C to  $200$  °C) have been fully characterized by the means of infrared spectroscopy. Transmission IR, ATR and Raman spectra were taken into account while making the assignment of the bands for both compounds. Many ambiguities concerning the origin of the bands and their assignment have been resolved. Recorded temperature-dependent spectra

enables following of the appearance/disappearance of the bands that may be correlated with the bands assignment.

### Supplementary material

Tables with summarized assignment of transmission IR spectra for MAI and FAI, Raman spectra of the samples.

**Acknowledgement.** The financial support was from the BAS-MANU Collaborative Project “Structural characteri-



zation and investigation of electrical and catalytic properties of new synthesized inorganic and organic-inorganic complex perovskites”.

## REFERENCES

- [1] L. K. Ono, E. J. Juarez-Perez, Y. Qi, Progress on perovskite materials and solar cells with mixed cations and Halide Anions, *ACS Appl. Mater. Interfaces.*, **9**, 30197–30246 (2017). <https://doi.org/10.1021/acsami.7b06001>.
- [2] J. Navas, A. Sánchez-Coronilla, J. J. Gallardo, N. Cruz Hernández, J. C. Piñero, R. Alcántara, C. Fernández-Lorenzo, D. M. De los Santos, T. Aguilar, J. Martín-Calleja, New insights into organic–inorganic hybrid perovskite  $\text{CH}_3\text{NH}_3\text{PbI}_3$  nanoparticles. An experimental and theoretical study of doping in  $\text{Pb}^{2+}$  sites with  $\text{Sn}^{2+}$ ,  $\text{Sr}^{2+}$ ,  $\text{Cd}^{2+}$  and  $\text{Ca}^{2+}$ , *Nanoscale.*, **7**, 6216–6229 (2015). <https://doi.org/10.1039/C5NR00041F>.
- [3] G. E. Eperon, S. D. Stranks, C. Menelaou, M. B. Johnston, L. M. Herz, H. J. Snaith, Formamidinium lead trihalide: A broadly tunable perovskite for efficient planar heterojunction solar cells, *Energy Environ. Sci.*, **7**, 982–988 (2014). <https://doi.org/10.1039/c3ee43822h>.
- [4] J. Breternitz, F. Lehmann, S. A. Barnett, H. Nowell, S. Schorr, Role of the iodide-methylammonium interaction in the ferroelectricity of  $\text{CH}_3\text{NH}_3\text{PbI}_3$ , *Angew. Chemie Int. Ed.* (2019). <https://doi.org/10.1002/anie.201910599>.
- [5] A. Cabana, C. Sandorfy, The infrared spectra of solid methylammonium halides, *Spectrochim. Acta.*, **18** 843–861 (1962). [https://doi.org/10.1016/0371-1951\(62\)80089-7](https://doi.org/10.1016/0371-1951(62)80089-7).
- [6] E. Castellucci,  $\beta$  and  $\gamma$  crystal forms of methylammonium chloride: polarized light infrared spectra and Raman spectra; Infrared spectra of matrix isolated methylammonium ion, *J. Mol. Struct.*, **23**, 449–461 (1974). [https://doi.org/10.1016/0022-2860\(74\)87013-4](https://doi.org/10.1016/0022-2860(74)87013-4).
- [7] A. Théorêt, C. Sandorfy, The infrared spectra of solid methylammonium halides-II, *Spectrochim. Acta Part A Mol. Spectrosc.*, **23**, 519–542 (1967). [https://doi.org/10.1016/0584-8539\(67\)80310-6](https://doi.org/10.1016/0584-8539(67)80310-6).
- [8] O. Yamamuro, M. Oguni, T. Matsuo, H. Suga, Calorimetric and dilatometric studies on the phase transitions of crystalline  $\text{CH}_3\text{NH}_3\text{I}$ , *J. Chem. Thermodyn.*, **18** 939–954 (1986). [https://doi.org/10.1016/0021-9614\(86\)90152-7](https://doi.org/10.1016/0021-9614(86)90152-7).
- [9] M. Mączka, A. Ciupa, A. Gağor, A. Sieradzki, A. Pikul, B. Macalik, M. Drozd, Perovskite Metal Formate Framework of  $[\text{NH}_2\text{-CH}^+\text{-NH}_2]\text{Mn}(\text{HCOO})_3$ : Phase Transition, Magnetic, Dielectric, and Phonon Properties, *Inorg. Chem.* **53** (2014) 5260–5268. <https://doi.org/10.1021/ic500479e>.
- [10] K. Hills-Kimball, Y. Nagaoka, C. Cao, E. Chaykovsky, O. Chen, Synthesis of formamidinium lead halide perovskite nanocrystals through solid-liquid-solid cation exchange, *J. Mater. Chem. C*, **5**, 5680–5684 (2017). <https://doi.org/10.1039/c7tc00598a>.
- [11] K. Mencil, P. Durlak, M. Rok, R. Jakubas, J. Baran, W. Medycki, A. Ciżman, A. Piecha-Bisiorek, Widely used hardly known. An insight into electric and dynamic properties of formamidinium iodide, *RSC Adv.* **8**, 26506–26516 (2018). <https://doi.org/10.1039/c8ra03871f>.
- [12] O. Yamamuro, M. Oguni, T. Matsuo, H. Suga, P-T phase relations of methylammonium halides, *Thermochim. Acta.*, **98**, 327–338 (1986). [https://doi.org/10.1016/0040-6031\(86\)87103-9](https://doi.org/10.1016/0040-6031(86)87103-9).
- [13] H. Ishida, R. Ikeda, D. Nakamura,  $^1\text{H}$  NMR studies on the reorientational motions of cations in four solid phases of methylammonium iodide and the self-diffusion of ions in its highest-temperature solid phase, *Bull. Chem. Soc. Jpn.*, **59**, 915–924 (1986). <https://doi.org/10.1246/bcsj.59.915>.
- [14] H. Ishida, R. Ikeda, D. Nakamura, Pre-melting state of methylammonium iodide as revealed by proton magnetic resonance, *Phys. Status Solidi.*, **70**, 151–154 (1982). <https://doi.org/10.1002/pssa.2210700261>.
- [15] A. A. Petrov, E. A. Goodilin, A. B. Tarasov, V. A. Lazarenko, P. V. Dorovatovskii, V. N. Khrustalev, Formamidinium iodide: Crystal structure and phase transitions, *Acta Crystallogr. Sect. E Crystallogr. Commun.*, **73** (2017) 569–572. <https://doi.org/10.1107/S205698901700425X>.
- [16] K. M. Boopathi, M. Ramesh, P. Perumal, Y. C. Huang, C. S. Tsao, Y. F. Chen, C. H. Lee, C. W. Chu, Preparation of metal halide perovskite solar cells through a liquid droplet assisted method, *J. Mater. Chem. A.*, **3**, 9257–9263 (2015). <https://doi.org/10.1039/c4ta06392a>.
- [17] M. Bukleski, S. Dimitrovska-Lazova, V. Makrievski, S. Aleksovska, A simple approach for determination of the phase transition temperature using infrared temperature-induced isosbestic points, *Spectrochim. Acta. Part A Mol. Spectrosc.*, in prep. (n.d.) 1–15.
- [18] N. Pellet, P. Gao, G. Gregori, T. Y. Yang, M. K. Nazeeruddin, J. Maier, M. Grätzel, Mixed-organic-cation perovskite photovoltaics for enhanced solar-light harvesting, *Angew. Chemie – Int. Ed.*, **53**, 3151–3157 (2014). <https://doi.org/10.1002/anie.201309361>.
- [19] E. Kucharska, J. Hanuza, A. Ciupa, M. Mączka, L. Macalik, Vibrational properties and DFT calculations of formamidinium-templated Co and Fe formates, *Vib. Spectrosc.*, **75**, 45–50 (2014). <https://doi.org/10.1016/j.vibspec.2014.09.001>.
- [20] O. Yamamuro, T. Matsuo, H. Suga, W. I. F. David, R. M. Ibberson, A. J. Leadbetter, Neutron diffraction and calorimetric studies of methylammonium iodide, *Acta Crystallogr. Sect. B.*, **48**, 329–336 (1992). <https://doi.org/10.1107/S0108768192000260>.
- [21] T. Glaser, C. Müller, M. Sendner, C. Krekeler, O. E. Semonin, T. D. Hull, O. Yaffe, J. S. Owen, W. Kowalsky, A. Pucci, R. Lovrinčić, Infrared spectroscopic study of vibrational modes in methylammonium lead halide perovskites, *J. Phys. Chem. Lett.*, **6**, 2913–2918 (2015). <https://doi.org/10.1021/acs.jpcclett.5b01309>.
- [22] A. Möller, J. George, R. Dronskowski, First full structural characterization of chloro formamidinium salts, *Zeitschrift Fur Anorg. Und Allg. Chemie.*, **644**, 1485–1491 (2018). <https://doi.org/10.1002/zaac.201800164>.

- [23] G. Bator, R. Jakubas, J. Baran, H. Ratajczak, Infrared studies of structural phase transitions in  $(\text{CH}_3\text{NH}_3)_3\text{Bi}_2\text{I}_9$  (MAIB), *J. Mol. Struct.*, **325**, 45–51 (1994).  
[https://doi.org/10.1016/0022-2860\(94\)80016-2](https://doi.org/10.1016/0022-2860(94)80016-2).
- [24] L. Wang, K. Wang, B. Zou, Pressure-induced structural and optical properties of organometal halide perovskite-based formamidinium lead bromide, *J. Phys. Chem. Lett.*, **7**, 2556–2562 (2016).  
<https://doi.org/10.1021/acs.jpcclett.6b00999>.
- [25] T. K. K. Srinivasan, M. Mylrajan, Phase transitions in  $\text{CH}_3\text{NH}_3\text{ClO}_4$  and  $\text{CH}_3\text{ND}_3\text{ClO}_4$ , *Phase Transitions.*, **38**, 97–113 (1992).  
<https://doi.org/10.1080/01411599208203466>.
- [26] J. T. Edsall, H. Scheinberg, Raman spectra of amino acids and related compounds V. Deuterium substitution in the amino group, *J. Chem. Phys.*, **8**, 520–525 (1940).  
<https://doi.org/10.1063/1.1750705>.
- [27] M. Mylrajan, T. K. K. Srinivasan, Raman and infrared spectra of phase transition in  $\text{CH}_3\text{NH}_3\text{ClO}_4$ , *J. Mol. Struct.* **143**, 105–108 (1986).  
[https://doi.org/10.1016/0022-2860\(86\)85215-2](https://doi.org/10.1016/0022-2860(86)85215-2).